Secondary Structure Forming Propensity Coupled with Amphiphilicity Is an Optimal Motif in a Peptide or Protein for Association with Chaperonin 60 (GroEL)†

Monika Preuss, Jonathan P. Hutchinson,‡ and Andrew D. Miller*

Imperial College Genetic Therapies Centre, Department of Chemistry, Imperial College of Science, Technology and Medicine, South Kensington, London SW7 2AY, U.K.

Received February 11, 1999; Revised Manuscript Received May 27, 1999

ABSTRACT: The interactions of GroEL with six dansyl peptides were investigated by means of our previously established fluorescence binding assay [Hutchinson, J. P., Oldham, T. C., El-Thaher, T. S. H., and Miller, A. D. (1997) *J. Chem. Soc., Perkin Trans. 2,* 279−288]. Three peptides (AMPH series) were constructed with a hierarchy of α-helix-forming propensities and amphiphilic characteristics. The remaining three peptides (NON-AMPH series) were prepared with a reordered amino acid sequence designed to form peptides of differing non-amphiphilic α-helix-forming propensity. Of these six peptides, two ($AMPH^+$ and $NON\text{-}AMPH^+$) were *N*-capped with an S-form α-helix-inducing template (Ro 47-1615, Hoffmann-La Roche), two ($AMPH^-$ and $NON\text{-}AMPH^-$) were *N*-capped with an R-form non-inducing template (Ro 47-1614, Hoffmann-La Roche), and two ($AMPH^R$ and $NON\text{-}AMPH^R$) were without *N*-cap modification. This paper describes how the known strength of interaction of an unfolded protein substrate with the molecular chaperone GroEL (K_d micromolar to nanomolar) may be emulated with a single peptide ($AMPH^+$) (apparent K_d 5 nM) which has a high propensity to form an amphiphilic α-helical structure in solution. Secondary structure forming propensity is not, in and of itself, an important contributor to the strength of interaction with GroEL. However, secondary structure forming propensity coupled with amphiphilicity may be sufficient to account for most, if not all, of the interaction strength between GroEL and an unfolded peptide or protein substrate.

Molecular chaperones, according to definition, are proteins whose function is to mediate the folding/refolding of other proteins without becoming part of the final folded structure. Of all the known molecular chaperones, perhaps the best characterized are the *Escherichia coli* (*E. coli*) molecular chaperone chaperonin 60 (Cpn60;[1] GroEL) and its co-molecular chaperone co-chaperonin 10 (Cpn10; GroES) (*1*−*19*). As a result, it is now well established that GroEL is a dynamic homo-oligomer comprising 14 subunits (each 57 259 Da; total molecular mass 801 626 Da) arranged in two stacked rings of 7 subunits each, while GroES consists of 7 subunits (each 10 368 Da; total molecular mass 72 576 Da) arranged in a single ring. Both GroEL and GroES have been extensively characterized by electron microscopy (*2*−*11*), and the X-ray crystal structures of GroEL (*12*, *13*), GroES (*14*), and a ternary complex between GroEL, GroES, and ADP (*15*) are also available. The cycle of interactions between GroEL, GroES, ATP, and an unfolded protein leading to assisted folding of the substrate is still a matter of some debate, but a consensus now appears to be emerging (*15*−*19*).

One of our principal research interests has been to understand the basis of the molecular recognition and binding of an unfolded protein substrate by GroEL. The association of substrates with GroEL is somewhat paradoxical in being both tight but at the same time promiscuous (*20, 21*), which underlines the fact that molecular recognition and binding of an unfolded substrate protein by GroEL is almost certainly not a phenomenon determined by specific amino acid sequences but rather one determined by more general structural features common to all unfolded protein substrates. In our previous work concerning substrate recognition and binding, we developed a fluorescence binding assay to observe and characterize the interaction of five *N*-dansyl peptides with GroEL (*1*). Our conclusions from this investigation were that general forces (in particular, hydrophobic interactions supplemented by electrostatic interactions) were the primary source of binding energy between GroEL and a substrate protein irrespective of whether the substrate protein was recognized and initially bound in the form of a random coil, a molten globule state, a late folding intermediate, or indeed a misfolded protein (*22*−*36*). Our results also suggested that within the structure of an unfolded or partially folded substrate protein, amino acid residue sequences combining hydrophobic residues with either polar neutral

† M.P. and J.P.H. thank the DAAD, BBSRC, and Roche Products Ltd. for financial support for research studentships. We thank the Mitsubishi Chemical Corp. for supporting the Imperial College Genetic Therapies Centre.

* Corresponding author. Tel: +44 171 594 5773. Fax: +44 171 594 5803. E-mail: a.miller@ic.ac.uk.

‡ Present address: Division of Physical Biochemistry, National Institiute for Medical Research, The Ridgeway, London NW7 1AA, U.K.

[1] Abbreviations: Cpn60 (GroEL), chaperonin 60; Cpn10 (GroES) cochaperonin 10; Fmoc, (9-fluorenyl)methoxycarbonyl; dansyl, 5-(dimethylamino)-l-naphthalenesulfonyl; tBu, *tert*-butyl; Boc, *tert*-butyloxycarbonyl; Mtt, 4-methyltrityl; DCC, dicyclohexylcarbodiimide; HOBt, hydroxybenzotriazole; TFA, trifluoroacetic acid; AU, arbitrary units.

10.1021/bi990342l CCC: $18.00
Published on Web 07/22/1999

and/or cationic residues would interact with GroEL under conditions of physiological salt strength, while sequences which were either exclusively polar or negatively charged would not. These conclusions have been supported by the results of others who have been variously investigating the interaction of single amino acids (*37*), peptides (*38*−*43*), protein fragments (*40*, *44*−*46*), and entire proteins (*27*, *29*, *31*, *44*, *46*−*50*) with GroEL. The importance of hydrophobic interactions to binding between GroEL and substrate proteins has been further supported by observations (*39*, *51*) which suggest that unfolded substrate proteins associate with sets of hydrophobic amino acid residues in GroEL, which are clustered in high density on the inside surface of the apical domains of each GroEL subunit (*12*, *13*, *15*).

Secondary structural elements (such as α-helices or *β*-sheets) would offer convenient, reasonably flexible three-dimensional scaffolds by means of which amino acid residue sequences, combining hydrophobic residues with either polar neutral and/or cationic residues, could interact with corresponding sets of amino acid residues in GroEL. The potential importance of secondary structure in molecular recognition and binding was originally suggested by observations made several years ago that GroEL can induce α-helical conformations in short peptides (*41*, *42*). These observations led to the proposal that α-helices could be a motif for GroEL molecular recognition. Latter, some evidence to show that α-helices and *β*-sheet structures may play a role in GroEL molecular recognition has also been advanced (*38*, *45*, *52*, *53*). By contrast, other research groups have suggested that secondary structural elements may not be so important to the processes of molecular recognition and binding (*27*, *31*, *54*). Without doubt, the issues concerning the potential involvement of secondary structure in molecular recognition and binding processes may be further complicated by the dynamic nature of the interaction between GroEL and a substrate protein once initial molecular recognition and binding have taken place. A number of research groups have looked at the conformations of structurally well-characterized substrate proteins bound to GroEL and have made several widely different conclusions depending upon the nature of the substrate protein and the binding conditions involved (*25*, *30*−*36*, *55*−*57*).

In this paper we shall describe the results of experiments performed using a set of six well-defined, 14-mer peptides designed to evaluate the relative importance of secondary structure forming propensity and amphiphilicity in the process of molecular recognition and binding of substrates by GroEL. What made this peptide approach attractive to us was the fact that 14-mer peptides would normally be too short to adopt a stable fold without assistance. Therefore, we considered that our peptides would be able to act as mimetics for unfolded substrate proteins while circumventing the complication of kinetic competition between substrate protein folding and binding to GroEL. Also, complications introduced by the dynamic nature of GroEL−substrate protein interactions would be reduced when studying the interaction of peptides, as opposed to proteins, with GroEL. Alternatively, we could be more sure of being able to focus upon the processes of initial molecular recognition and binding without undue added complications. Using our six peptides, we come to the main conclusion that peptide subdomains of a protein substrate which have a propensity to form polar neutral and/or cationic amphiphilic secondary structures would be capable of mediating the majority, if not the whole, of the molecular recognition and binding between a substrate protein and GroEL. Our studies suggest that secondary structure forming propensity coupled with amphiphilicity should be considered an optimal motif in a peptide or substrate protein for initial molecular recognition followed by binding of a substrate protein by GroEL.

MATERIALS AND METHODS

Materials. All chemicals used were of analytical grade or better and were obtained from Sigma Chemical Co., Dorset, U.K. Pig heart mMDH (as an ammonium sulfate suspension) was obtained from Boehringer-Mannheim, U.K. Deionized distilled MilliQ water was used throughout. UV−visible absorption measurements were made on an Amersham Pharmacia Biotech Ultrospec III at ambient temperature. Circular dichroism spectra were obtained on a Jasco J-720 spectropolarimeter fitted with a thermostated cuvette holder. Fluorescence assays were performed on a Shimadzu RF 5001PC spectrofluorophotometer, fitted with a thermostated cuvette holder, using monochromator bandwidths of 5 or 10 nm. Non-linear regression analysis of all data sets was performed using Grafit version 3.0, Erithacus Software Ltd., Staines, U.K.

Preparation of Homogeneous GroEL and GroES. All GroEL and GroES concentrations refer to the homo-oligomer concentrations. GroEL was initially purified from a recombinant strain of *E. coli* according to previously published methods (*58*). Following this, GroEL was further purified in the following manner (*59*). In brief, after elution from Q-Sepharose, GroEL-containing fractions were combined and dialyzed against 20 mM Tris-HCl, pH 7.6, containing 1 mM *β*-ME and 5 mM $MgCl_2$ (buffer B). This GroEL-containing solution (10 mL, approximately 10 mg/mL of protein) was then supplemented with 5 mM KCl and 2 mM ATP and dialyzed for a further 1 h at ambient temperature against 20 mM Tris-HCl, pH 7.6, containing l mM *β*-ME, 5 mM $MgCl_2$, 5 mM KCl, and 2 mM ATP (buffer A). GroEL was then loaded at flow rate of 1.5 mL/min onto a column of Reactive Red 120 agarose (type 3000-CL) (2.6 × 30 cm) which had been preequilibrated with buffer A. After 30 min had elapsed following loading, the column was washed with buffer A (200 mL) and then eluted with a linear gradient (400 mL) of 0−100% buffer B at a flow rate of 1.5 mL/min. Elution was monitored at 280 nm and fractions (15 mL) were collected on ice. Fractions containing essentially tryptophan-free GroEL were combined, concentrated (Amicon N_2-pressure concentrator, 100K membrane, Filtron), and dialyzed against 50 mM Tris-HCl, pH 7.6, containing 2 mM DTT and stored for short periods at 4 °C. For longer term storage, GroEL solutions were supplemented with glycerol (50% v/v) and stored either at −20 °C without freezing or at −50 °C following rapid freezing in liquid nitrogen.

GroES was also initially purified from a recombinant strain of *E. coli* according to previously published methods (*58*). Following this, GroES was further purified in the following manner. After elution from Q-Sepharose, GroES-containing fractions were combined and dialyzed against 50 mM Tris-HCl, pH 8.5, containing 0.75 M $(NH_4)_2SO_4$ and 2 mM EDTA (buffer C) at 4 °C. Aliquots (2 mL, approximately 7.5 mg/

mL of protein) were then loaded at a flow rate of 1.5 mL/min onto a column of high-performance Phenyl-Sepharose (2.6 × 12 cm) which had been previously equilibrated with buffer C at ambient temperature. The column was then eluted with a linear gradient (120 mL) of 0−100% 50 mM Tris-HCl, pH 8.5, containing 2 mM EDTA (buffer D) using a flow rate of 3 mL/min. Elution was monitored at 280 nm and fractions (2 mL) were collected on ice. GroES-containing fractions (50−70% buffer D) were identified by SDS−PAGE and then combined and concentrated (Amicon N_2-pressure concentrator, 30K membrane, Filtron) to a minimum volume (1 mL) before dialysis against buffer B at 4 °C. This GroES-containing solution was then loaded at a flow rate of 1 mL/min onto a column of Reactive Red 120 agarose (type 3000-CL) (1.0 × 15 cm) which had been pre-equilibrated at ambient temperature with buffer B. The column was then eluted isocratically with buffer B using a flow rate of 1 mL/min. Elution was monitored at 280 nm and fractions (1 mL) were collected on ice. Fractions containing GroES were identified by SDS−PAGE and then combined, concentrated (Amicon N_2-pressure concentrator, 30K membrane, Filtron), and dialyzed against 50 mM Tris-HCl, pH 7.6, containing 2 mM DTT and stored as described for the GroEL protein. The Reactive Red columns were regenerated by washing with deionized water in order to release tryptophan-containing impurities.

After preparation, the concentrations of GroEL and GroES in the stored stock solutions were determined by quantitative amino acid analysis. The ability of homogeneous GroEL and GroES to function as molecular chaperones was then compared with standard gel filtration/ion-exchange prepared GroEL and GroES using our mitochondrial malate dehydrogenase folding assay system (*23*, *58*).

Peptide Preparation. The six dansyl peptides used in this study were prepared as follows. An AMPH precursor peptide was synthesized by Peptide Products Ltd., Wiltshire, U.K. A NON-AMPH precursor peptide was synthesized and supplied on the resin by Affinity Research Products Ltd., Devon, U.K. The AMPH precursor peptide was supplied with the sequence *N*-ALY$K_{(Fmoc)}K_{(Fmoc)}$II$K_{(Fmoc)}K_{(Fmoc)}$-LLES$K_{(Dansyl)}$-*C* and the NON-AMPH precursor peptide with the sequence *N*-$A_{(Fmoc)}LY_{(tBu)}K_{(Boc)}IK_{(Boc)}K_{(Boc)}IK_{(Boc)}$-$LLE_{(t-Bu)}S_{(t-Bu)}K_{(Mtt)}$-resin.

The $AMPH^+$ peptide was prepared as follows. The S-form α-helix-inducing template (Ro 47-1615, Hoffmann-La Roche) (11 mg) (Figure 2) was activated by treatment with dicyclohexylcarbodiimide (DCC) (1 mol equiv, 69 μL of a 352 mM solution in dimethylformamide), hydroxybenzotriazole (HOBt) (32 mg, 10 mol equiv), and diisopropylethylamine (0.1 mol equiv, 4 μL of a 10% v/v solution in dimethylformamide). After 1 h at ambient temperature, dichloromethane (100 μL) was added followed, after a further 1 h, by the AMPH precursor peptide (71 mg) in dimethylformamide (3 mL) containing diisopropylethylamine (10 mol equiv). The mixture was sonicated for 2 min at 40 °C to dissolve the precursor peptide and then stirred at ambient temperature for 18 h. After evaporation to dryness, the residue was shaken with piperidine (20% v/v) in dimethylformamide (4 mL) for 2 h at ambient temperature and then evaporated to dryness. Crude $AMPH^+$ peptide was dissolved with sonication in aqueous TFA (0.1% v/v), containing acetonitrile (20% v/v), and then eluted using the same water−solvent mixture through a P2 Bio-Gel column (2 × 22 cm), attached to an FPLC system (Amersham Pharmacia Biotech, U.K), at a flow rate of 1 mL/min. Elution was monitored at 280 nm, and peptide-containing fractions were then combined and freeze-dried. Finally, $AMPH^+$ was purified to homogeneity by preparative reversed-phase chromatography using a PepRPC HR10/10 column attached to a FPLC system (Amersham Pharmacia Biotech, U.K). The column was equilibrated with aqueous TFA (0.1% v/v), containing acetonitrile (10% v/v), and peptide was then eluted at a flow rate of 2 mL/min with a 10−100% linear gradient (80 mL) of acetonitrile, containing TFA (0.1% v/v). Elution was monitored at 280 nm and peak fractions were collected, combined, and freeze-dried. Peptide identity was confirmed by fast atom bombardment mass spectrometry. The $AMPH^-$ peptide was prepared using the R-form non-inducing template (Ro 47-1614, Hoffmann-La Roche) in a manner identical to that of the $AMPH^+$ peptide. The $AMPH^R$ peptide was obtained as an uncoupled byproduct of the above series of reactions after elution of either crude $AMPH^+$ or $AMPH^-$ peptides through the reversed-phase chromatography column.

$NON\text{-}AMPH^+$, $NON\text{-}AMPH^-$, and $NON\text{-}AMPH^R$ peptides were prepared from the resin-attached NON-AMPH precursor peptide by the following sequence of deprotection and chemical coupling steps. Initially, the resin (140 mg) was incubated for 1 h with shaking at ambient temperature in dimethylformamide (10 mL), containing TFA (1% v/v), washed with dichloromethane (1 mL aliquots), and dried in vacuo. Removal of the Mtt-protecting group was monitored by the ninhydrin test (Applied Biosystems Ltd.). Usually a second cycle of deprotection was required to ensure complete removal of the Mtt-protecting group. After this, the resin was repeatedly washed with dimethylformamide (1 mL aliquots), suspended in dimethylformamide (2 mL), containing dansyl chloride (10 mol equiv) and diisopropylethylamine (10 mol equiv), and then incubated for 1 h with shaking at ambient temperature at which point dansylation of the *C*-terminal lysine residue was complete. Next, the resin was freed of residual reagents by repeated washing with dimethylformamide (1 mL aliquots) until all coloration was removed, then further washed with dichloromethane (1 mL aliquots), and dried in vacuo. Resin could be stored at this stage in anhydrous conditions at −20 °C. $NON\text{-}AMPH^+$ peptide was prepared in the following way. The stored resin was resuspended in dimethylformamide (10 mL), containing piperidine (25% v/v), and incubated for 1 h with shaking to remove the *N*-terminal Fmoc-protecting group from the resin-bound dansylated peptide. Following this, the resin was repeatedly washed with dimethylformamide (1 mL aliquots) and then dichloromethane (1 mL aliquots) and dried in vacuo. Next, the resin was resuspended in dimethylformamide (1 mL), containing the S-form template (Ro 47-1615) (4.6 mg, 1 mol equiv) (Figure 2), HOBt (14.5 mg, 10 mol equiv), and DCC (107 μL of a 1 M solution in 1-methyl-2-pyrrolidinone, 10 mol equiv). The mixture was incubated at ambient temperature for 24 h with shaking. The resin was subjected to repeated washes with dimethylformamide (1 mL aliquots) and then dichloromethane (1 mL aliquots) and finally dried in vacuo. Peptide was liberated from the resin and fully deprotected by resuspending the above resin in 95% aqueous TFA and incubating for 2 h with shaking at ambient temperature. Free peptide was separated from the solid phase

by filtration through a small pad of glass wool and finally precipitated in ice-cold methyl *tert*-butyl ether (40 mL). The precipitate was recovered by centrifugation (2500*g*) and the pellet washed repeatedly with ice-cold methyl *tert*-butyl ether to remove residual reagents. Crude NON-AMPH$^+$ peptide was resuspended in aqueous TFA (0.1% v/v), and acetonitrile, containing TFA (0.1% v/v), was added until the peptide dissolved. After freeze-drying, crude NON-AMPH$^+$ was then redissolved in aqueous TFA (0.1% v/v) and purified to homogeneity by preparative reversed-phase chromatography using the PepRPC HR10/10 column as above. The column was equilibrated with aqueous TFA (0.1% v/v), and peptide was then eluted at a flow rate of 2 mL/min with a 0−100% linear gradient (80 mL) of acetonitrile, containing TFA (0.1% v/v). Elution was monitored at 280 nm, and peak fractions were collected manually and freeze-dried. Peptide identity was confirmed by fast atom bombardment mass spectrometry. The NON-AMPH$^-$ peptide was prepared in a way almost identical to that of the NON-AMPH$^+$ peptide except that the R-form template (Ro 47-1614) was used in place of the S-form template (Ro 47-1615) (Figure 2). The NON-AMPH^R peptide was prepared similarly except that the template addition step was not performed. Furthermore, an undansylated version of this peptide was prepared in which the dansyl group addition step was not carried out. Analytical reversed-phase chromatography was performed on a C-18 Vydac column (4.6 mm × 15 cm) attached to a Gilson HPLC apparatus. Elution was monitored at 226 nm. Peptides were eluted at a flow rate of 1 mL/min with a 0−100% linear gradient of acetonitrile, containing TFA (0.1% v/v), and found to be essentially homogeneous (>95%).

Concentrated stocks of all six *C*-dansyl peptides were prepared in dimethyl sulfoxide and stored in aliquots at −20 °C. *C*-Dansyl peptide concentrations were determined spectrophotometrically in 6 M guanidinium chloride, pH 7.0, using an extinction coefficient, ϵ_{330}, of 4100 M^{-1} cm^{-1} originally measured for dansylglycine (*60*). Concentrations of undansylated peptides were determined by weight.

Circular Dichroism Spectroscopy. Solutions (approximately 200 μM) of all six peptides were prepared in 20 or 50 mM Tris-HCl buffer, pH 7.6 (at ambient temperature), at 20 °C. The stock solutions were then diluted 5-fold, 25-fold, and 100-fold with deionized water, and peptide spectra were recorded in the far-UV and near-UV regions after 18 h of equilibration at 20 °C in the dark. Far-UV spectra were acquired at 20 °C using 0.02, 0.1, 0.5, and 2.0 cm path-length quartz cells for the stock solutions and the dilutions, respectively. Near-UV spectra were measured using the 0.5 cm path-length quartz cell. A total of four scans were averaged to obtain each spectrum, after which the appropriate buffer background was subtracted.

Aggregation Assays. In a first set of aggregation assays, stock solutions of all six peptides in 50 mM Tris-HCl buffer, pH 7.6, at 20 °C, containing 2 mM DTT (assay buffer), were diluted in the same buffer to a final concentration of 3.0 or 0.5 μM. Dansyl group fluorescence emission intensities at 500 nm were monitored using a spectrofluorometer over a period of 24 h at 20 °C. The excitation wavelength was 350 nm. Readings were made at 2 min intervals, and the excitation shutter was closed between readings in order to minimize photobleaching of the dansyl group. Excitation and emission bandwidths were set at 5 nm. In a second set of aggregation assays, stock solutions of all six peptides in assay buffer were diluted to concentrations ranging from 10 nM to 2 μM in the same buffer. Solutions were then incubated at 20 °C for 18 h in the dark before the fluorescence emission intensity was measured at 500 nm on excitation at 350 nm. Excitation and emission bandwidths were 10 nm.

Fluorescence Binding Assays. Prior to use in binding studies, GroEL solutions were extensively dialyzed at 4 °C against 50 mM Tris-HCI buffer, pH 7.6, containing 2 mM DTT (assay buffer), and concentrated in 100 kDa cut-off Centricon concentrators (Amicon, MA) to approximately 50−75 μM. NON-AMPH$^+$, NON-AMPH$^-$, and NON-AMPH^R peptides were each diluted to a concentration of 1.0 μM and equilibrated for 18 h at 20 °C in the dark prior to use. In the case of these peptides, the titrations were performed using single peptide solutions as described previously (*1*). Peptide solutions (1.0 μM) were titrated with GroEL from 6 nM to 2 μM. At each addition, the dansyl fluorescence emission spectrum was recorded between 450 and 600 nm, using an excitation wavelength of 350 nm and excitation/emission bandwidths of 10 nm. In the case of the AMPH$^+$, AMPH$^-$, and AMPH^R peptides, individual solution aliquots, each containing peptide at a fixed concentration (0.5 μM), were equilibrated with different concentrations of GroEL in the range from 6 nM to 2 μM. After 18 h at 20 °C in the dark, individual fluorescence emission intensities at 500 nm were measured using an excitation wavelength of 350 nm and excitation/emission bandwidths of 10 nm.

Fluorescence emission intensities at 500 nm, corrected for GroEL background, were tabulated, and the emission intensity of free peptide at 500 nm (i.e., in the absence of GroEL) was subtracted in order to give the fluorescence intensity enhancement, ΔI_{500}, due to interaction of the given peptide with GroEL at each individual GroEL concentration. ΔI_{500} data were then analyzed as a function of the GroEL concentration using a model for binding in which a given peptide was assumed to be able to interact with an unspecified number of independent binding sites on the GroEL homo-oligomer. This model was used previously (*1*) to derive the expression:

$$\Delta I_{500} = (\Delta\Phi[P]_t[G]_t K_a)/(1 + [G]_t K_a) \qquad (1)$$

where $[P]_t$ is the total peptide concentration, $[G]_t$ the total GroEL concentration, ΔI_{500} the fluorescence intensity enhancement at 500 nm, K_a the apparent association constant, and $\Delta\Phi$ a term deriving from fluorescence quantum yield enhancement upon peptide binding to GroEL. The origins of these terms, the theoretical basis, and a validation of the binding model have been described previously (*1*, *61*).

In one instance, a reversed binding experiment was performed in which a solution of GroEL (10 nM) in assay buffer was titrated with NON-AMPH^R peptide from 10 nM to 50 μM. The fluorescence emission intensity from a separate set of protein-free control titrations was recorded in parallel to determine the contribution to the observed fluorescence emission intensity of the peptide alone.

GroES Competition Experiments. GroES in assay buffer was concentrated in 30 kDa cut-off Centricon concentrators (Amicon, MA) to approximately 100 μM prior to use. B_{amph} (*1*), NON-AMPH$^+$, NON-AMPH$^-$, and NON-AMPH^R peptides (1 μM) were then each separately pre-incubated with

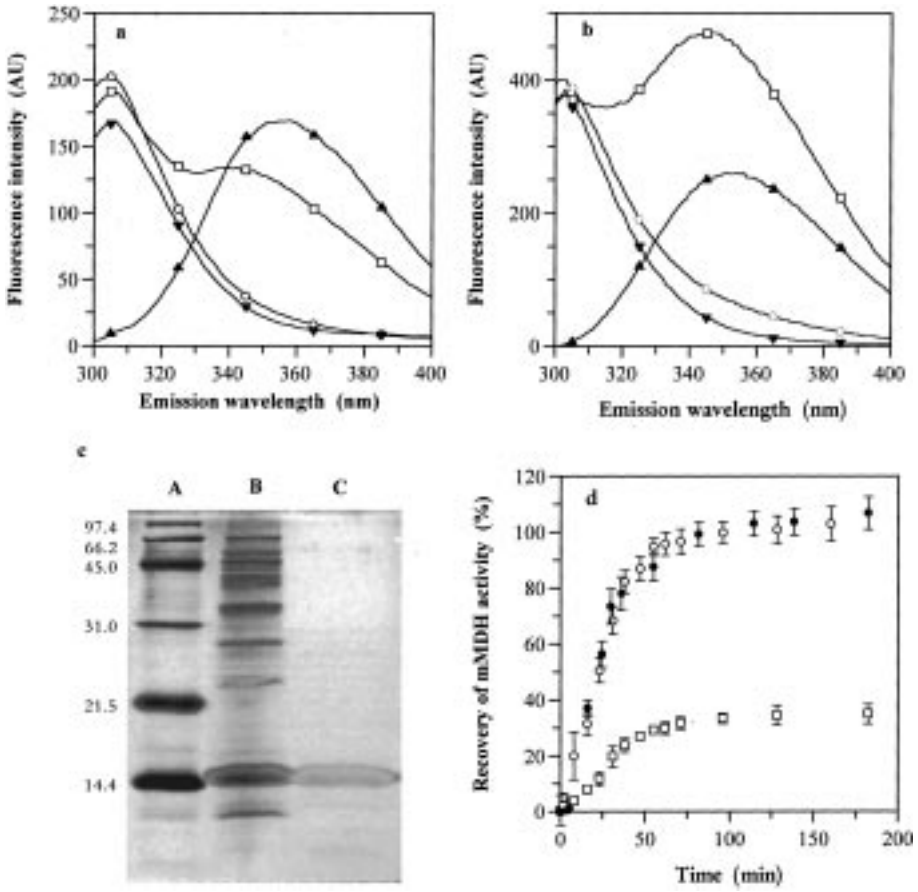

FIGURE 1: (a) Fluorescence emission spectra of GroEL. Ion-exchange purified GroEL ($GroEL_{std}$) (□) and Reactive Red purified GroEL ($GroEL_{RR}$) (○), both at 0.5 μM, are shown. Reference spectra of *N*-acetyltryptophanamide (▲) and L-tyrosine (▼) are also illustrated. Protein and amino acid spectra were obtained after 1 h incubation in 6 M guanidinium chloride, pH 7.0, and 30 mM β-mercaptoethanol in 50 mM Tris-HCl, pH 7.6, and corrected for guanidinium chloride buffer background. Such spectra were used to calculate the tryptophan content (measured at 354 nm) of GroEL according to calibration curves derived from the fluorescence emission intensities of standard solutions of *N*-acetyltryptophanamide (1−20 μM) (*89*). Excitation wavelengths for all spectra shown were 280 nm; excitation and emission band widths were 5 nm. (b) Fluorescence emission spectra of GroES. Ion-exchange purified GroES ($GroES_{std}$) (□) and Reactive Red purified GroES ($GroES_{RR}$) (○), both at 5.0 μM, are shown. *N*-Acetyltryptophanamide (▲) and L-tyrosine (▼) reference spectra are also illustrated. The tryptophan content was assessed as in (a). (c) Overloaded silver-stained 15% SDS−polyacrylamide gel showing molecular weight markers (lane A), $GroES_{std}$ (2.5 μM) (lane B), and $GroES_{RR}$ (2.5 μM) (lane C). (d) Refolding of mitochondrial malate dehydrogenase (mMDH) spontaneously (□), with the assistance of $GroEL_{std}$ and $GroES_{std}$ (○) and with the assistance of $GroEL_{RR}$ and $GroES_{RR}$ (●). The error bars give the deviation from the mean of two independent experiments. Assays were performed according to previously published protocols (*23*, *58*).

GroEL for several minutes at 20 °C in assay buffer. GroEL concentrations were fixed near the K_d value of the peptide−GroEL interaction (i.e., 75 nM for NON-AMPH$^+$ and NON-AMPH$^-$ peptides; 200 nM for NON-AMPH^R and B_{amph} peptides). GroES was then titrated from 10 nM to 2.0 μM in small aliquots. A second set of experiments was performed in the presence of 125 mM $MgCl_2$. In this case, GroEL concentrations were 0.5 μM throughout. GroES was titrated from 50 nM to 10 μM (maximum allowed before significant inner-filter effects were suspected). Finally, a third set of experiments was conducted with the addition of 10 mM KCl and 8 mM ATP (125 mM $MgCl_2$). This concentration of ATP was sufficient to maintain the ATPase activity at a saturating rate throughout the titration experiment. In the case of all three sets of experiments, changes in fluorescence emission intensity at 500 nm, ΔI_{500}, were observed as a function of the GroES concentration. Emission intensities were corrected for GroEL and GroES background.

Peptide Competition Experiments. NON-AMPH^R (1 μM) was pre-incubated with GroEL (0.5 μM) for several minutes at 20 °C in assay buffer. This mixture was subsequently titrated with undansylated NON-AMPH^R peptide from a concentration of 10 nM to 100 μM. The change in fluorescence emission intensity at 500 nm, ΔI_{500}, was measured as a function of the undansylated NON-AMPH^R peptide concentration. Emission intensities were corrected for peptide and GroEL background.

RESULTS

GroEL and GroES Purification and Functional Characterization. Over the past few years, there has been great concern expressed over the purity of GroEL and GroES used in various mechanistic studies, most especially concerning the presence of tryptophan-containing impurities in samples of both proteins (*47*, *62*−*65*). For this reason we developed purification procedures which would ensure the absence of these tryptophan-containing impurities. Accordingly, GroEL was prepared using a standard gel filtration/ion-exchange procedure (*58*) and then further purified by elution through a Reactive Red dye binding column. Clark et al. (*47*) were the first to describe the use of this dye binding column in their purification of the GroEL protein. However, we found

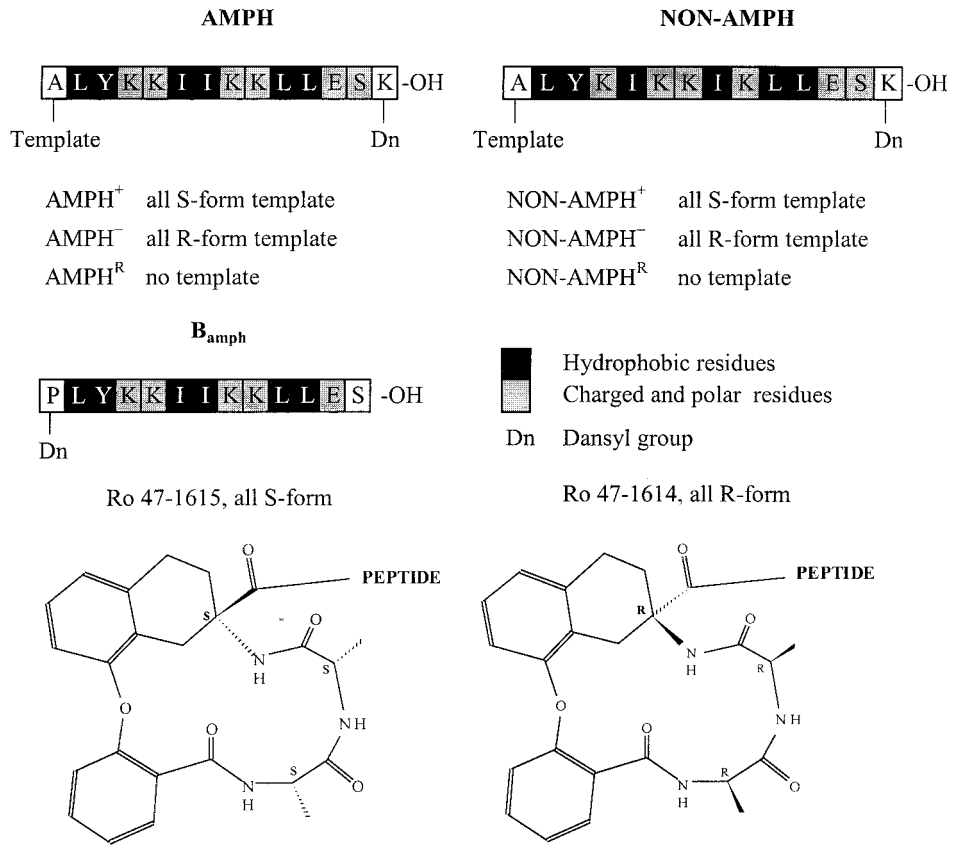

FIGURE 2: Illustration of the sequences of the AMPH and NON-AMPH series peptides used in the work described in this paper. The B_{amph} peptide sequence is included for comparison (*1*). Also included are the structures of the S-form α-helix-inducing template (Ro 47-1615) and the R-form non-inducing template (Ro 47-1614) developed by Hoffmann-La Roche (*68*).

it necessary to adapt their procedure by introducing ATP into the elution buffer in order to release GroEL-associated peptide/protein impurities into the buffer for separation. In our hands without this added ATP, significant GroEL-associated impurities remained which could be observed as supernumerary bands on SDS−polyacrylamide gels. Combined and concentrated GroEL-containing fractions from the Reactive Red column were analyzed by fluorescence spectroscopy (Figure 1a) and found to possess a minimal tryptophan content (<0.05 mol of tryptophan/mol of GroEL oligomer). The homogeneity of this GroEL preparation was further demonstrated by amino acid analysis and SDS−polyacrylamide gel electrophoresis (using overloaded silver-stained gels). The results of these two analyses have been presented elsewhere (*59*).

GroES was initially prepared using the same gel filtration/ion-exchange procedure used in the preparation of GroEL (*58*), but two additional column elution steps then proved necessary to remove as much of the tryptophan-containing impurities as possible. In the first step, GroES was bound to and eluted from a hydrophobic interaction (HIC) column using a procedure adapted from Burston et al. (*66*), yielding GroES which showed the presence of residual tryptophan fluorescence. In the second step, purification was accomplished by elution through a Reactive Red dye binding column in the absence of ATP, after which the GroES containing fractions were combined and concentrated. The resulting stock solution was analyzed by fluorescence spectroscopy (Figure 1b) and found to possess minimal tryptophan content (<0.07 mol of tryptophan/mol of GroES oligomer). SDS−polyacrylamide gel electrophoresis analysis (using overloaded silver-stained gels, Figure 1c) revealed GroES to be essentially homogeneous. Gratifyingly, GroEL and GroES prepared according to the above procedures were found to be fully functional as molecular chaperone and co-chaperone, respectively, in our standard mitochondrial malate dehydrogenase refolding assay system (*23*, *58*) (Figure 1d).

Peptide Sequences. The interactions of six different peptides with GroEL were investigated. The six peptides studied may be divided into two main series of peptides: those containing the amphiphilic AMPH amino acid residue sequence (Figure 2) (i.e., $AMPH^+$, $AMPH^-$, and $AMPH^R$) and those containing the non-amphiphilic NON-AMPH amino acid residue sequence (Figure 2) (i.e., $NON\text{-}AMPH^+$, $NON\text{-}AMPH^-$, and $NON\text{-}AMPH^R$). The AMPH series peptide sequence was derived directly from the basic amphiphilic (B_{amph}) peptide used in our previous GroEL-peptide binding studies (Figure 2) (*1*), the sequence of which corresponds to the 13 *C*-terminal α-helical residues of human platelet factor 4 precursor (*67*). The AMPH series sequence was designed to have alternating pairs of positively charged lysine (K) residues with hydrophobic isoleucine (I) and leucine (L) residues which would dispose to form an amphiphilic α-helix in the event that an α-helical conformation were adopted in solution by this peptide sequence. The helical wheel and ribbon structures of the AMPH series peptide sequence should serve to illustrate this design principle (panels a and b of Figure 3, respectively). The ability of $AMPH^+$ and $AMPH^-$ to form α-helices in solution was controlled by the incorporation of an *N*-cap template, namely an S-form α-helix-inducing template (Ro 47-1615) in the case of $AMPH^+$ and an R-form non-inducing template

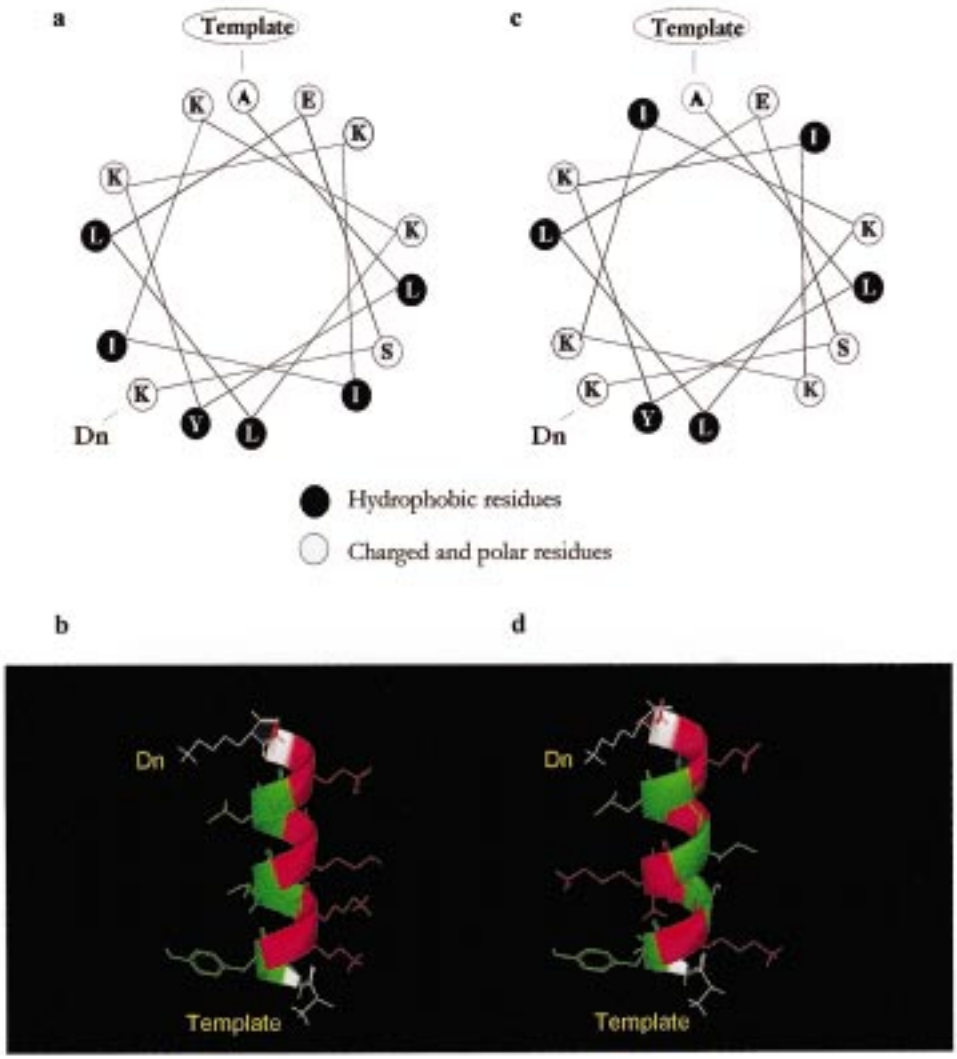

FIGURE 3: Helical wheel diagrams of AMPH (a) and NON-AMPH (c) series peptides together with computer-generated images of α-helical structures of AMPH (b) and NON-AMPH (d). The helical conformation was modeled from the peptide sequences using Quanta version 97 (Molecular Simulations), and the images were constructed from these coordinates using WebLab version 3.1 (Molecular Simulations). Hydrophobic residues are marked in green, and polar/charged residues are shown in red.

(Ro 47-1614) in the case of $AMPH^{-}$ (Figure 2). The S-form template was originally designed by Abrecht et al. (*68*) of Hoffmann-La Roche AG (Switzerland) to adopt a low-energy conformation which mimics the first turn of an α-helix, placing four C═O hydrogen bond acceptors in a parallel arrangement ideal to complement the first four N−H hydrogen bond donor groups belonging to the first four peptide bonds of an attached peptide comprised of natural L-(S)-amino acid residues. Normally, peptides are not thought to form α-helical structures with ease in solution unless these first four peptide bonds are complemented by intramolecular hydrogen bond formation. This is because the energy released from formation of these hydrogen bonds is thought to be required to overcome the entropic barrier to α-helix formation. The corresponding R-form template was designed as a control template whose three stereocenters are in the opposite configuration to the S-form template and should therefore be unable to nucleate α-helical secondary structure in an attached peptide composed of L-(S)-amino acid residues (*68*). In the case of the $AMPH^{R}$ peptide, no *N*-terminal modification was carried out.

The non-amphiphilic NON-AMPH series peptides were prepared to provide a direct comparison with the amphiphilic AMPH series peptides. The NON-AMPH series peptide sequence is a reordered version of the AMPH sequence and was therefore intended to form a non-amphiphilic α-helix in the event that an α-helical conformation were adopted in solution. This design principle is illustrated by the corresponding helical wheel and ribbon structure diagrams (panels c and d of Figure 3, respectively). In the case of the $NON\text{-}AMPH^{+}$ and $NON\text{-}AMPH^{-}$ peptides, the ability of either to form α-helical conformations in solution was controlled by attached S-form and R-form *N*-cap templates, respectively (Figure 2). All six AMPH and NON-AMPH series peptides were labeled with a 5-(dimethylamino)-1-naphthalenesulfonyl [dansyl (Dn)] group attached to the N^{ϵ}-atom of the *C*-terminal lysine residue to act as a fluorescent reporter of binding interactions with GroEL. Before use, all peptide structures were verified by fast atom bombardment mass spectrometry, and homogeneity was verified by analytical reversed-phase chromatography.

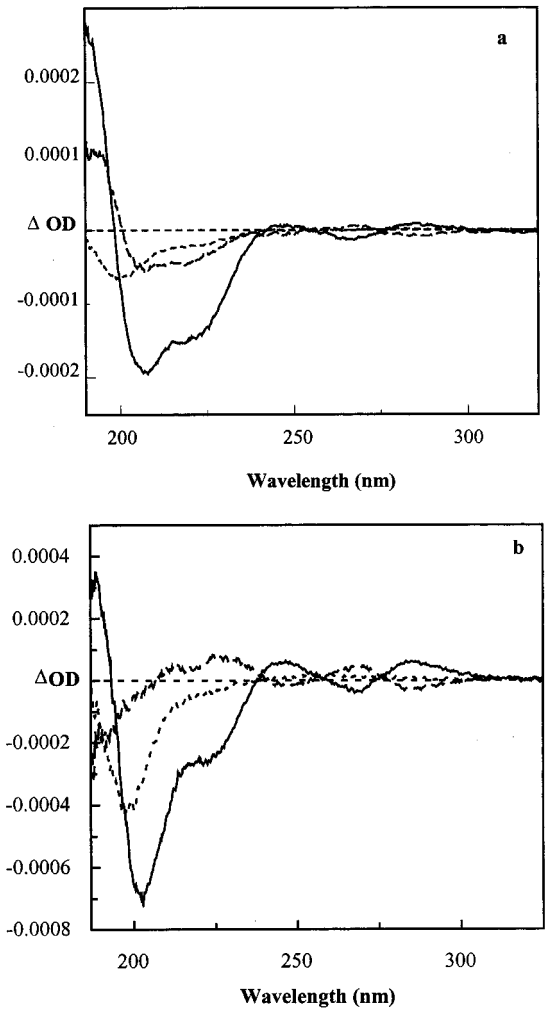

FIGURE 4: Far-UV circular dichroism spectra of AMPH and NON-AMPH series peptides. (a) Spectra of $AMPH^+$ (—) (52 μM), $AMPH^-$ (— —) (39 μM), and $AMPH^R$ (- - -) (120 μM) were recorded in 50 mM Tris-HCl, pH 7.6, at 20 °C following 18 h incubation at 20 °C. Spectra were recorded in a 0.02 cm path-length cell and are the result of four acquisitions which were baseline corrected. Spectra were normalized to a concentration of 52 μM. (b) Spectra of NON-$AMPH^+$ (—) (198 μM), NON-$AMPH^-$ (— —) (176 μM), and NON-$AMPH^R$ (- - -) (193 μM) were recorded in 20 mM Tris-HCl, pH 7.6, at 20 °C following 18 h incubation at 20 °C. Spectra were recorded as in (a) and normalized to a concentration of 198 μM.

Circular Dichroism Spectroscopy of Peptides. Circular dichroism (CD) spectroscopy of all six peptides was performed in order to determine secondary structure forming propensity in solution before GroEL binding experiments were carried out. The secondary structure forming propensity of all three AMPH series peptides (i.e., $AMPH^+$, $AMPH^-$, and $AMPH^R$) was much as anticipated. The $AMPH^+$ peptide showed a clear propensity to form α-helical structures in solution (Figure 4a). By contrast, the $AMPH^-$ peptide exhibited considerably less α-helical character in solution, while the untemplated $AMPH^R$ peptide appeared to be completely unstructured (Figure 4a). A similar hierarchy of behavior was observed with the three NON-AMPH series peptides. NON-$AMPH^+$ showed significant α-helical character in solution but mixed with unstructured conformations, while both the NON-$AMPH^-$ and NON-$AMPH^R$ peptides were completely unstructured (Figure 4b). Peptides with a propensity to form amphiphilic helices may readily form helical bundles or aggregates in solution. The formation of such bundles may even potentiate helix formation by stabilizing helical conformations through interpeptide interactions (*69*−*71*). Such features have been exploited previously in the de novo design of proteins (*69*). This stabilization of helical conformations through helical bundle formation of amphiphilic peptides may explain why the $AMPH^+$ peptide exhibited more helical character in solution than its non-amphiphilic NON-$AMPH^+$ counterpart. Nevertheless, as far as we were able to determine by CD spectroscopy, the relative α-helix-forming propensities of both the $AMPH^+$ and NON-$AMPH^+$ peptides were maintained qualitatively even at the lowest concentrations analyzed (1−2 μM), where aggregation effects appeared to be minimal (see below).

Aggregation Assays. Two aggregation assays were performed. In the first, stock solutions of each peptide were diluted to 3 and 0.5 μM, and time-dependent changes in fluorescence emission intensity were monitored. In each case, the time required for complete relaxation of fluorescence emission intensity after dilution was of the order of 6−10 h, a result that was attributed to slow aggregate dissociation after dilution (results not shown). This information was used to design a second aggregation experiment in which stock solutions of each peptide were diluted to concentrations ranging from 10 nM to 2 μM and the fluorescence emission intensity was monitored after 18 h incubation at 20 °C (Figure 5). All three AMPH series peptides appeared to show similar fluorescence emission behavior up to a concentration of 0.5 μM. Thereafter, $AMPH^+$, and to a much lesser extent $AMPH^-$, showed a more enhanced fluorescence emission intensity with increasing concentration. We presumed that this enhanced fluorescence emission intensity was caused by concentration-dependent aggregation of these peptides. This seemed reasonable to us since $AMPH^+$, and to a lesser extent $AMPH^-$, had been demonstrated previously by CD spectroscopy (Figure 4) to have propensities to form amphiphilic α-helical structures in solution, which would themselves be likely to aggregate above a certain critical concentration into self-stabilizing structures (see above). Therefore, subsequent fluorescence binding assays were performed using a fixed peptide concentration of 0.5 μM, at which concentration the tendency to aggregation of the peptides was presumed to be minimal. As might be expected, all three NON-AMPH series peptides appeared to show similar fluorescence emission behavior up to a higher concentration of 1.0 μM. Thereafter, the NON-$AMPH^+$ peptide showed some divergence in fluorescence behavior. Therefore, NON-AMPH peptide fluorescence binding assays were performed using a fixed peptide concentration of 1.0 μM. The apparently lower tendency of NON-$AMPH^+$ to self-associate as compared to $AMPH^+$ is consistent with the observed trends in secondary structure forming propensity (Figure 4).

Fluorescence Binding Assays. The analysis of peptide binding to GroEL was performed using our own fluorescent peptide binding assay (*1*). In brief, excitation of the *C*-dansyl peptides in free solution at 350 nm typically resulted in a weak fluorescence emission maximum near 540 nm. Upon interaction with increasing amounts of GroEL, the peptide fluorescence was characterized by a blue-shift in the emission maximum toward 500 nm and an increase in fluorescence

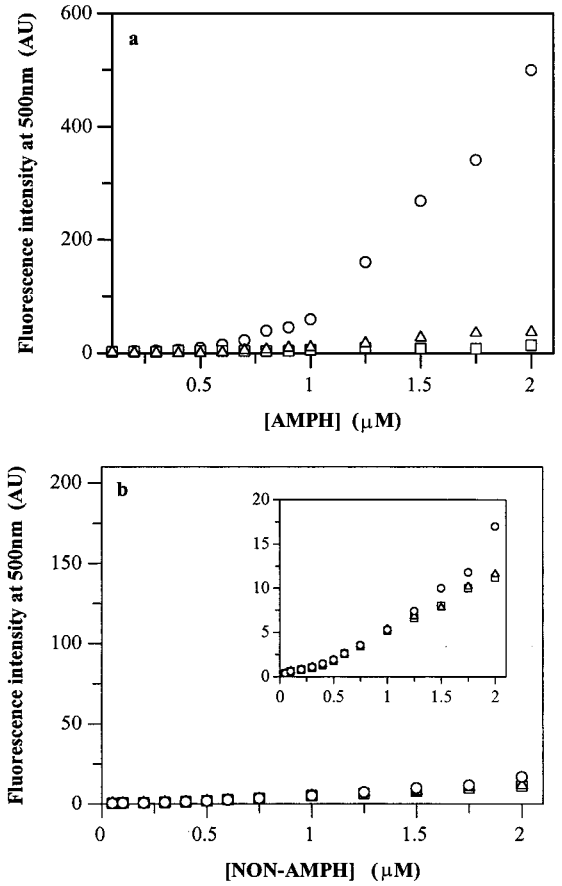

FIGURE 5: Fluorescence emission intensities of AMPH and NON-AMPH series peptides as a function of the peptide concentration. (a) Emission intensities of $AMPH^+$ (○), $AMPH^-$ (△), and $AMPH^R$ (□) peptides were measured at the given concentrations in assay buffer after 18 h incubation at 20 °C. Fluorescence emission intensities were measured at 500 nm on excitation at 350 nm. (b) Emission intensities of NON-$AMPH^+$ (○), NON-$AMPH^-$ (△), and NON-$AMPH^R$ (□) peptides were measured in the same way as for (a).

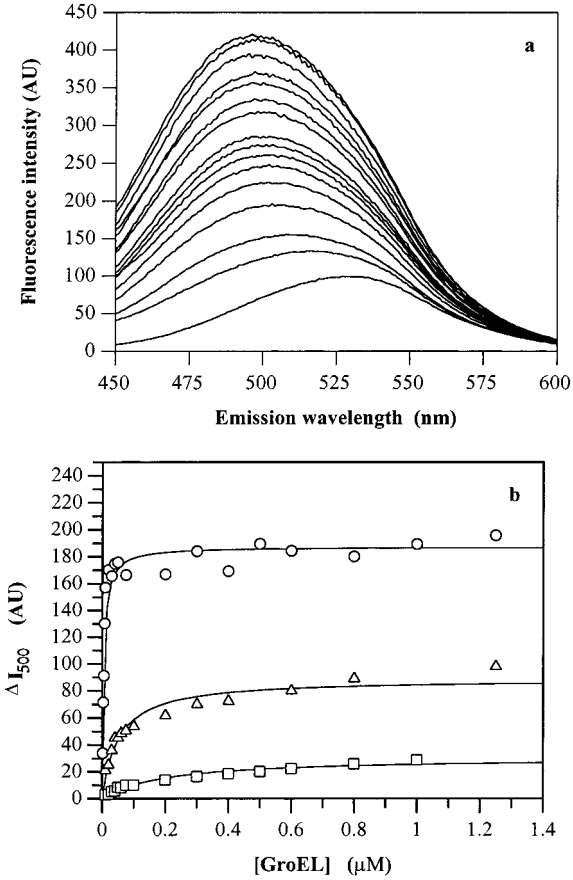

FIGURE 6: Peptide GroEL binding assay. (a) Representative sequence of dansyl group fluorescence emission spectra following the titration at 20 °C of a fixed concentration of NON-$AMPH^+$ peptide (1 μM) with GroEL (from 6 nM to approximately 2 μM) in assay buffer. Excitation was performed at 350 nm. (b) AMPH series peptide binding isotherms were generated by plotting the corrected change in fluorescence intensity at 500 nm, ΔI_{500}, against the GroEL concentration for $AMPH^+$ (○), $AMPH^-$ (△), and $AMPH^R$ (□) peptides (all peptides were 0.5 μM). Lines through the data are a two-parameter fit to eq 1 to yield the apparent association constants, K_a.

intensity which tended toward saturation with increasing GroEL concentration (Figure 6a). In the absence of interaction no such blue-shift and fluorescence intensity increase were observed (*1*). The strength of binding interaction was assessed by plotting the fluorescence intensity enhancement at 500 nm, ΔI_{500}, corrected for GroEL background, against the GroEL concentration. Binding parameters were obtained by a two-parameter fit of the data to expression 1 with $\Delta\Phi$ and K_a as variables (Figure 6b).

Table 1 shows a series of GroEL binding data expressed as apparent dissociation constants ($K_d = 1/K_a$) obtained at 20 °C for all six peptides in standard buffer, 50 mM Tris-HCl, pH 7.6, and 2 mM DTT (assay buffer). Temperature-dependent free energy changes of binding at 20 °C, $\Delta G(T)_{bind}$, were obtained using the equation:

$$\Delta G(T)_{bind} = -RT \ln K_a \qquad (2)$$

where K_a is the apparent association constant and R is the molar gas constant (8.314 J mol^{-1} K^{-1}). Both the $AMPH^R$ and NON-$AMPH^R$ peptides were found to bind to GroEL with affinities very similar to the parent B_{amph} peptide, under similar binding conditions (*1*). By contrast, the $AMPH^-$ and NON-$AMPH^-$ peptides bound to GroEL approximately 4- and 3-fold more tightly than the respective untemplated peptides ($AMPH^R$ and NON-$AMPH^R$). Interestingly, the helical NON-$AMPH^+$ peptide bound to GroEL with an affinity similar to that of its nonhelical variant NON-$AMPH^-$. By contrast, the helical $AMPH^+$ peptide was observed to bind to GroEL with an affinity almost two orders of magnitude greater than that of the corresponding untemplated peptide $AMPH^R$ and approximately one order of magnitude greater than that of the other templated peptides (Table 1).

Table 1: Apparent Dissociation Constants for Peptide−GroEL Interaction at 20 °C[a]

peptide	K_d at 20 °C (μM)	$\Delta G°_{bind}$ at 20 °C (kJ mol^{-1})
$AMPH^+$	0.005 ± 0.001	−46.6 ± 0.5
$AMPH^-$	0.051 ± 0.008	−41.0 ± 0.4
$AMPH^R$	0.196 ± 0.033	−37.7 ± 0.4
NON-$AMPH^+$	0.062 ± 0.002	−40.4 ± 0.1
NON-$AMPH^-$	0.083 ± 0.003	−39.7 ± 0.1
NON-$AMPH^R$	0.215 ± 0.007	−37.5 ± 0.1

[a] Dissociation constants K_d (μM) were determined in assay buffer (50 mM Tris-HCl, pH 7.6, 2 mM DTT). K_d values were calculated according to eq 1; errors were derived from the standard errors of the fit of the binding isotherms.

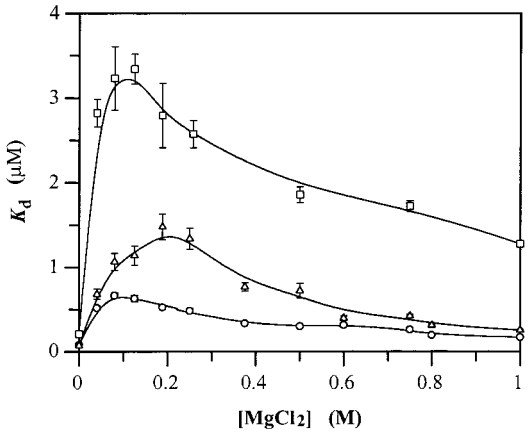

FIGURE 7: Effect of magnesium chloride on the apparent dissociation constants for the interaction between NON-AMPH$^+$ (○), NON-AMPH$^-$ (△), or NON-AMPH^R (□) with GroEL. Each point represents the result of an individual peptide−GroEL titration experiment, as described in the legend to Figure 6, and was performed at the indicated concentrations of $MgCl_2$. Error margins were derived from the standard errors of the fit of the binding curves. The lines through the data were generated with a spline function.

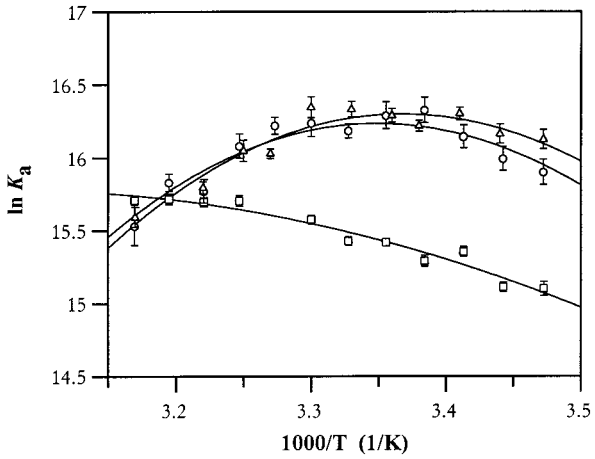

FIGURE 8: Van't Hoff plots to show the effect of temperature on the apparent association constants, K_a, for the interaction between the NON-AMPH$^+$ (○), NON-AMPH$^-$ (△), or NON-AMPH^R (□) peptides with GroEL. Each point represents the result of an individual peptide−GroEL titration experiment performed at the indicated temperature as described in the legend to Figure 6. Error margins were derived from the standard errors of the fit of the binding isotherms. Lines through the data show a three-parameter fit to eq 3 from which the thermodynamic parameters given in Table 2 were derived.

The effect of magnesium chloride ($MgCl_2$) ionic strength on the interaction of the NON-AMPH$^+$, NON-AMPH$^-$, and NON-AMPH^R peptides with GroEL was investigated and is summarized in Figure 7 where the binding interaction, measured in terms of K_d, is plotted as a function of the concentration of $MgCl_2$. Finally, the effect of temperature on the binding of the NON-AMPH$^+$, NON-AMPH$^-$, and NON-AMPH^R peptides with GroEL was investigated. The results obtained [over the temperature range 10 to 42 °C (i.e., 283 to 315 K)] are shown in the form of van't Hoff plots (Figure 8). Thermodynamic parameters were derived from these plots using a truncated form of the integrated van't Hoff equation (3) and eqs 4−6 (*72*):

$$\ln K_a = a + b(1/T) + c \ln T \quad (3)$$

$$\Delta C_{p\ \mathrm{bind}} = Rc \quad (4)$$

$$\Delta H(T)_{\mathrm{bind}} = R(cT - b) \quad (5)$$

$$\Delta S(T)_{\mathrm{bind}} = [\Delta H(T)_{\mathrm{bind}} - \Delta G(T)_{\mathrm{bind}}]/T \quad (6)$$

where $\Delta C_{p\ \mathrm{bind}}$ is the change in specific heat capacity for peptide binding (under the conditions of pH, ionic strength, ambient pressure, and fixed peptide concentration used in the binding assays), while $\Delta H(T)_{\mathrm{bind}}$ and $\Delta S(T)_{\mathrm{bind}}$ are the temperature-dependent enthalpy change and entropy change of peptide binding, respectively. The calculated parameters for all three peptides are summarized in Table 2. In the absence of GroEL, the fluorescence emission properties of all three NON-AMPH series peptides were found not to be affected by temperature (over the range 283 to 315 K) (results not shown). Therefore, we are confident that the observed and calculated thermodynamic data (Figure 8, Table 2) accurately reflect the nature of the interactions between the peptides and GroEL.

GroES and Peptide Competition Experiments. In order to provide additional validation for our peptide−GroEL binding experiments, the association between GroEL and the NON-AMPH series peptides and B_{amph} was investigated in the presence of GroES. Given the fact that the polypeptide binding regions of GroEL are well-known to double up as GroES binding sites (*15*, *39*, *51*), we intended to perform competition experiments to establish whether or not GroES could compete directly with the peptides for binding to GroEL. Prior to these studies, however, we were interested to see whether the peptides and GroES would interact with each other and performed binding experiments with GroES in place of GroEL. We were able to establish that the fluorescence emission intensities of the dansyl peptides were essentially independent of the concentration of GroES. This result would suggest, although not prove, that there was no significant interaction taking place between the peptides and GroES (results not shown). Following this, GroEL binding competition experiments were carried out in which individual mixtures of each peptide with GroEL were titrated with GroES and the change in fluorescence emission at 500 nm was observed as a function of the GroES concentration. There was a clear decline in fluorescence emission intensity of all peptides with increasing GroES concentration (Figure 9a), which suggested that the availability of peptide binding sites was being reduced in the presence of GroES. This process was promoted in the presence of a physiological concentration of salt ($MgCl_2$) (Figure 9b), probably as a result of salt screening of the electrostatic repulsion between the two acidic proteins GroEL and GroES (*73*), allowing them to associate more readily and deprive the peptides of their binding sites. This effect was substantially enhanced in the presence of $MgCl_2$, KCl, and ATP (Figure 9c), where the affinity between GroEL and GroES is known to be especially tight (reported K_d values between 16 and 26 nM) (*74*−*77*). These conditions may even lead to the formation of symmetrical "football"-shaped complexes in which all potential peptide binding sites would be occupied by GroES (*4*, *5*, *74*, *78*). ATP binding to GroEL and the resulting conformational changes in GroEL may also weaken GroEL−peptide interactions, particularly at high concentrations of nucleotide when all ATP binding sites are occupied (*7*, *10*, *11*, *79*−*81*).

Table 2: Thermodynamic Parameters for the NON-AMPH Series Peptide−GroEL Interactions[a]

		parameters at 20 °C		parameters at 37 °C	
peptide	$\Delta C_{p\ \mathrm{bind}}$ (kJ mol^{-1} K^{-1})	$\Delta H(T)_{\mathrm{bind}}$ (kJ mol^{-1})	$\Delta S(T)_{\mathrm{bind}}$ (J mol^{-1} K^{-1})	$\Delta H(T)_{\mathrm{bind}}$ (kJ mol^{-1})	$\Delta S(T)_{\mathrm{bind}}$ (J mol^{-1} K^{-1})
NON-AMPH^{+}	-4.54 ± 0.01	19.86 ± 2.3	202.0 ± 8.4	-33.06 ± 2.3	26.4 ± 8.3
NON-AMPH^{-}	-2.99 ± 0.01	14.04 ± 2.7	183.5 ± 8.8	-38.68 ± 2.7	7.9 ± 8.8
NON-AMPH^{R}	-0.81 ± 0.01	24.95 ± 1.7	212.8 ± 6.1	13.18 ± 1.7	173.4 ± 6.0

[a] Binding assays were performed over a range of temperatures in assay buffer. Thermodynamic parameters were obtained by van't Hoff analysis (Figure 8) of each set of temperature dependent K_a values.

A second set of competition experiments was carried out in which the interaction of GroEL and NON-AMPH^{R}, the least aggregation-prone peptide (see above), was measured in the presence of undansylated NON-AMPH^{R} in an attempt to ascertain whether peptide binding to GroEL was specific. A 50% complex formation inhibition was achieved at a ratio of labeled:unlabeled peptide $\approx$ 1:1, consistent with same-site competition (Figure 10).

DISCUSSION

In our previous work concerning the molecular recognition of peptides and proteins by GroEL, we established some principles of molecular recognition which govern the association of GroEL with peptides (*1*). These principles defined the optimal features of a peptide's amino acid primary sequence which are needed to promote association with GroEL, as well as those features which discourage binding. The work described in this paper represents our attempts to build upon our previous work in order to understand the importance of substrate secondary structure in the recognition and binding of peptides, and by extrapolation substrate proteins, to GroEL. Unfolded/non-native substrate proteins commonly possess exposed secondary structural elements; therefore, an investigation into the GroEL interaction of a set of peptides, some with secondary structure forming propensities, was expected to allow us to draw conclusions about the interaction of unfolded substrate proteins with GroEL as well. Our approach was to start from the peptide which had been found to bind to GroEL most tightly in our previous work, namely, an *N*-dansyl basic amphiphilic peptide (B_{amph}) (Figure 2). We then constructed six systematic variants of this peptide, the AMPH and NON-AMPH series peptides, which possessed a hierarchy of α-helix-forming propensities and amphiphilic characteristics (Figures 2 and 3). By studying the interaction of all six peptides with GroEL, we hoped that their relative strengths of interaction with GroEL would allow us to draw conclusions as to the relative importance of secondary structure and amphiphilicity in the process of molecular recognition and binding by GroEL. Prior to performing any binding studies, the secondary structure forming propensities of all six peptides were examined by CD spectroscopy and confirmed the expected hierarchy of α-helix-forming propensities with the AMPH^{+} and NON-AMPH^{+} peptides displaying strong helical features (Figure 4). On the basis of aggregation experiments (Figure 5), peptide−GroEL binding studies were then performed by titrating a fixed concentration of each peptide (0.5 μM in the case of AMPH series peptides and 1.0 μM in the case of NON-AMPH series peptides) with GroEL until the fluorescence emission intensity of each peptide reached saturation (Figure 6). Upon processing the fluorescence binding data, significant differences in the strengths of interaction of the amphiphilic and non-amphiphilic peptides with GroEL were observed (Figure 2, Table 1). Most importantly, the AMPH^{+} peptide, possessing the highest amphiphilic α-helix-forming propensity of the peptides, was found to bind to GroEL with much enhanced affinity when compared to the similarly α-helical non-amphiphilic NON-AMPH^{+} counterpart. In interpreting this important difference, we considered that the association of AMPH^{+} with GroEL was probably being promoted by the amphiphilic character of the α-helical secondary structure of this peptide. This suggestion was substantiated by the observation that both the NON-AMPH^{+} and NON-AMPH^{-} peptides bound with similar affinity to GroEL even though the former possessed α-helical character in solution while the latter apparently did not. This indicated that non-amphiphilic secondary structure forming propensity was not contributing to the strength of binding with GroEL.

Following these binding studies, experiments were performed to characterize the nature of the binding interactions between the six peptides and GroEL. In our previous work, the parent B_{amph} peptide had been found to bind to GroEL through a combination of hydrophobic and electrostatic interactions (*1*). Therefore, we expected that the six peptide variants of B_{amph} would bind to GroEL in a similar manner. In performing the binding studies described above, we observed consistently that interactions between the NON-AMPH series peptides and GroEL reached equilibrium within the mixing time of the experiment, while interactions between the AMPH series peptides (especially AMPH^{+}) and GroEL appeared to reach equilibrium more slowly [equilibration times of several hours were sometimes required (see Materials and Methods)]. As a result, we decided to focus our investigations on the NON-AMPH series peptides. The effect of $MgCl_2$ on the interaction of all three NON-AMPH peptides with GroEL was examined (Figure 7). The sensitivity to ionic strength displayed by all peptides suggested that binding was partly mediated through electrostatic interactions of the cationic peptides with the acidic GroEL protein (*73*), which were progressively weakened by increasing ionic strength causing binding affinities to lower. Following this, the increasing strength of hydrophobic interactions at higher ionic strengths allowed binding affinities to progressively increase again. Therefore, at first sight, the NON-AMPH series peptides appeared to be binding to GroEL by a combination of hydrophobic and electrostatic interactions similar to those of the parent B_{amph} peptide (*1*).

This suggestion was further reinforced by studies on the effect of temperature on the interaction of the NON-AMPH peptides with GroEL (Table 2, Figure 8). All three van't Hoff plots showed negative curvatures and correspondingly

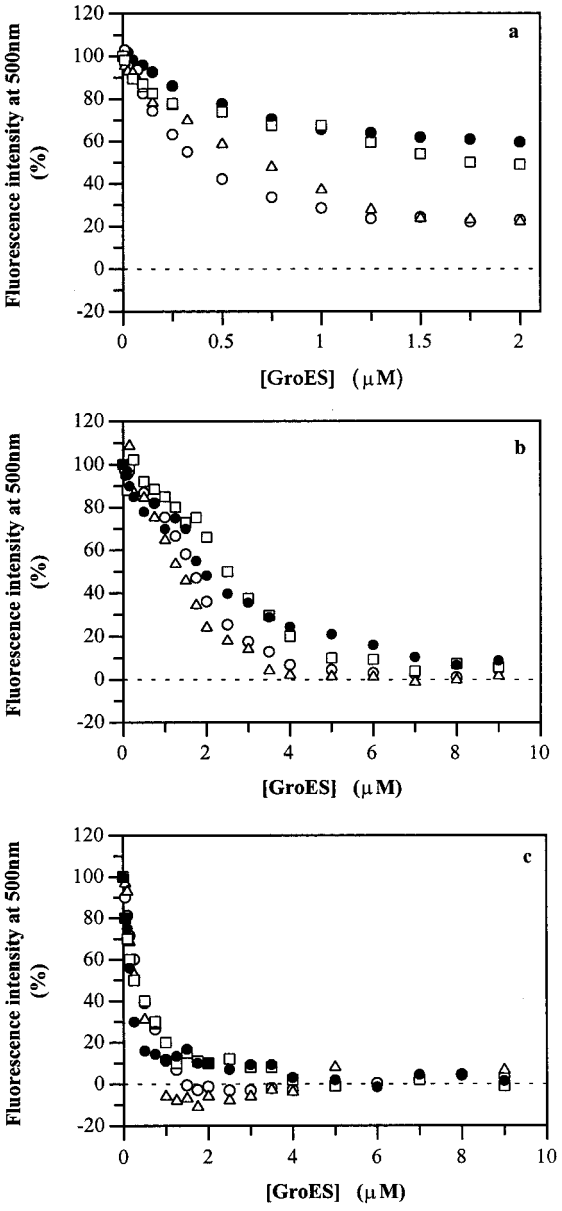

FIGURE 9: GroES competition experiments. Shown are percentage changes in fluorescence emission intensity at 500 nm of B_{amph} and NON-AMPH series peptide−GroEL mixtures as a function of the concentration of added GroES. B_{amph}, NON-AMPH$^+$, NON-AMPH$^-$, and NON-AMPH^R peptides (1 μM) were each separately pre-incubated with GroEL for several minutes at 20 °C before the addition of GroES. (a) Results obtained in assay buffer with B_{amph} (●) (0.2 μM GroEL), NON-AMPH^R (□) (0.2 μM GroEL), NON-AMPH$^-$ (△) (75 nM GroEL), and NON-AMPH$^+$ (○) (75 nM GroEL). (b) Results obtained using the same buffer as in (a) but containing 125 mM $MgCl_2$; the same symbols for peptides apply as in (a); GroEL concentrations were 0.5 μM with all mixtures. (c) Results obtained using the same buffer as in (b) but also containing 10 mM KCl and 8 mM ATP; the same symbols for peptides apply as in (a); GroEL concentrations were 0.5 μM in all mixtures.

negative values of $\Delta C_{p\ bind}$, indicative of hydrophobic interactions (*82*). Nevertheless, the relatively low value of $\Delta C_{p\ bind}$ (approximately −0.8 kJ mol^{-1} K^{-1}) measured for the interaction of the untemplated NON-AMPH^R peptide with GroEL was taken as evidence for a mode of binding in which hydrophobic interactions, which make negative contributions to $\Delta C_{p\ bind}$, are roughly balanced by positive contributions to $\Delta C_{p\ bind}$ from electrostatic interactions, leading to the dehydration of the protein interface and the release of electro-

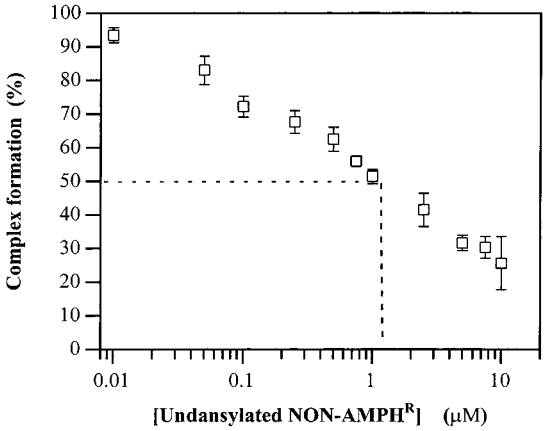

FIGURE 10: Peptide competition experiment. Shown are percentage changes in fluorescence emission intensity at 500 nm of *C*-dansyl NON-AMPH^R peptide−GroEL mixtures as a function of the concentration of added undansylated NON-AMPH^R. Measurements were made in assay buffer. *C*-Dansyl NON-AMPH^R (1 μM) was incubated with GroEL (0.5 μM) for several minutes at 20 °C before each addition of undansylated NON-AMPH^R.

restricted water (*83*, *84*). Similar values of $\Delta C_{p\ bind}$ between −1.8 and −0.2 kJ mol^{-1} K^{-1} have been reported for the interaction of GroEL with the moderately hydrophilic, denatured proteins α-casein (*85*) and pepsin (*86*), respectively. By contrast, the values of $\Delta C_{p\ bind}$ measured for the interaction of the templated peptides NON-AMPH$^+$ and NON-AMPH$^-$ were similar to values of −3.6 and −4.19 kJ mol^{-1} K^{-1} reported for the interaction of the hydrophobic molten globule and reduced states of α-lactalbumin (*29*, *86*) and denatured subtilisin with GroEL (*85*), respectively. It can be concluded, therefore, that, in the case of the binding of the templated peptides to GroEL, hydrophobic interactions appeared to be dominating over electrostatic interactions. This difference in the nature of the binding interaction between the templated and untemplated peptides appeared to point toward a contribution from the templates. Enhanced hydrophobic binding through a contribution by the templates would also offer an explanation as to why the templated peptides NON-AMPH$^+$ and NON-AMPH$^-$ bound to GroEL considerably tighter than the untemplated NON-AMPH^R peptide (Table 1). By extrapolation, the same argument would explain the increased affinity of AMPH$^-$ when compared to the untemplated AMPH^R peptide (Table 1). Given the similarities in the amino acid composition between the NON-AMPH and AMPH series peptides, it would seem reasonable to conclude that the AMPH peptides were binding to GroEL by a similar combination of hydrophobic and electrostatic interactions. This allows us to suggest an explanation for the especially high affinity of GroEL for the amphiphilic helical AMPH$^+$ peptide. An amphiphilic AMPH$^+$ helix would be able to present an organized but flexible three-dimensional array or cluster of hydrophobic residues on one face of the helix and cationic/polar neutral hydrophilic side chains on the other face (Figure 3). When interacting with GroEL, hydrophobic and electrostatic interactions would be promoted with corresponding arrays or clusters of residues at the polypeptide binding sites in GroEL. These binding sites are located at the inside surface of the apical domains of each GroEL subunit and are known to consist of sets of hydrophobic amino acid residues (*12*, *13*, *15*). Therefore, we would suggest that AMPH$^+$, displaying

a combination of secondary structure forming propensity coupled with amphiphilicity, was most probably interacting with GroEL via the cluster of hydrophobic amino acid side chains presented on one face of the $AMPH^+$ helix, although electrostatic interactions would also still be possible, too. Drawing from our equilibrium binding data, we are unable to investigate the possibility that initial recognition of peptides may be followed by conformational changes in both GroEL and its substrate which additionally drive the binding interaction. However, given the strong affinity of GroEL for the $AMPH^+$ peptide, the secondary structural characteristics of this peptide, and the structural nature of the GroEL peptide binding sites, we would suggest that few structural adjustments would be necessary to optimize the free energy of association between GroEL and the $AMPH^+$ peptide. Such suggestions as these would all be very much in keeping with the observations of Brazil et al. (*38*), Hlodan et al. (*45*), and others (*40, 52, 53*), not to mention the original pioneering work of Landry and Gierasch (*41, 42*).

Finally, an attempt was made to determine the approximate number of peptide binding sites on GroEL. According to our previously described model for peptide binding to GroEL, which was used to derive expression 1, the apparent association constant, K_a, was related to the individual association constants of one peptide with one individual GroEL binding site, κ_a according to the expression:

$$K_a = n\kappa_a \tag{7}$$

where n corresponds to the total number of peptide binding sites available on GroEL. In order to determine n, it was necessary to perform a peptide−GroEL binding study in which a fixed concentration of GroEL was titrated with *C*-dansyl peptide until the fluorescence emission intensity enhancement reached saturation. Due to the high number of peptide binding sites on GroEL, this required the titration with high concentrations of peptide, an experiment that could only be performed with $NON\text{-}AMPH^R$, which in contrast to the other peptides was found not to aggregate strongly. Therefore, a very low fixed concentration of GroEL (10 nM) was titrated with $NON\text{-}AMPH^R$ until the fluorescence emission intensity of the system appeared to be saturating. Data corresponding to the change in fluorescence emission intensity at 500 nm, ΔI_{500}, were then analyzed using expression 8, which is a variant of expression 1:

$$\Delta I_{500} = (\Delta\Phi[P]_t[G]_t\kappa_a)/(1 + [P]_tK_a) \tag{8}$$

Approximately 80% saturation of the fluorescence signal was achieved with this titration, allowing for a good fit of the experimental data to eq 8. The value of κ_d derived from this reversed titration of experiment was 16.28 ± 0.88 μM as compared to the apparent dissociation constant value (K_d) of 0.21 ± 0.01 μM, determined by the more usual procedure of titrating peptide with GroEL (effective concentration of binding sites $n[G]_t$) (Table 1). According to expression 7, the number of individual peptide binding sites on the GroEL oligomer was estimated at 77 ± 9. This result should be viewed with a little caution since the titration of a very low fixed concentration of GroEL with $NON\text{-}AMPH^R$ peptide resulted in a relatively small fluorescence intensity enhancement. This approach was necessary in order to maintain the concentration of peptide binding sites on GroEL below the value of the dissociation constant. Otherwise, deviations from the binding model, based on the assumption that the concentration of free ligand equals the concentration of total ligand in the system (*1*), would be expected.

The reported apparent dissociation constant, K_d, for the interaction of the $AMPH^+$ peptide with GroEL (Table 1) is of the same order of magnitude as reported dissociation constants of proteins and peptides from GroEL (nanomolar region) under very similar conditions (*23, 40, 55, 87, 88*) and even tighter than some reported dissociation constants (micromolar region) involving other GroEL−protein interactions (*29, 54, 85, 86*). This is remarkable given the fact that it has been suggested that there is a minimum threshold length of 55−65 amino acid residues necessary in a given protein in order for there to be a stable interaction between the substrate and GroEL (*45*). However, it is important to note that, according to the way in which the apparent dissociation constant, K_d, had to be measured in the above experiments, the actual dissociation constant, κ_d, for the interaction of $AMPH^+$ with any one, individual GroEL binding site may be up to 2 orders of magnitude larger (κ_d 0.39 μM) than the reported K_d, owing to the large number of peptide binding sites estimated on GroEL (77 ± 9). Moreover, the estimation of κ_d assumes that the interaction of a peptide with any one binding site is independent of all other such interactions. If positive cooperativity were occurring, as would be expected when an unfolded protein substrate comes into close proximity with GroEL, values for the dissociation constants of each peptide binding event would reduce rapidly. Therefore, we would propose that when an unfolded protein substrate is recognized by GroEL, tight binding should be possible through the cooperative interaction of GroEL with peptide subdomains in the substrate, particularly if these have a propensity to form polar neutral and/or cationic amphiphilic secondary structures (such as α-helices or β-sheets). In other words, these peptide subdomains of a protein substrate should be sufficient to mediate the majority of the interaction of a substrate protein with GroEL. Secondary structure forming propensity coupled with amphiphilicity in peptide subdomains of proteins should therefore be considered optimal motifs for molecular recognition and binding of substrate peptides or proteins by GroEL.

ACKNOWLEDGMENT

We thank Dr. Daniel Obrecht of Hoffmann-La Roche AG, Switzerland, for providing us with samples of the two *N*-cap templates Ro 47-1615 and Ro 47-1614.

REFERENCES

1. Hutchinson, J. P., Oldham, T. C., El-Thaher, T. S. H., and Miller, A. D. (1997) *J. Chem. Soc., Perkin Trans. 2,* 279−288.
2. Hendrix, R. W. (1979) *J. Mol. Biol. 129,* 375−392.
3. Chandrasekhar, G. N., Tilly, K., Woolford, C., Hendrix, R., and Georgopoulos, C. (1986) *J. Biol. Chem. 261,* 12414−12419.
4. Azem, A., Kessel, M., and Goloubinoff, P. (1994) *Science 265,* 653−656.
5. Schmidt, M., Rutkat, K., Rachel, R., Pfeifer, G., Jaenicke, R., Viitanen, P., Lorimer, G., and Buchner, J. (1994) *Science 265,* 656−659.

6. Engel, A., Hayer-Hartl, M. K., Goldie, K. N., Pfeifer, G., Hegerl, R., Müller, S., da Silva, A. C. R., Baumeister, W., and Hartl, F.-U. (1995) *Science 269*, 832−836.
7. Roseman, A. M., Chen, S., White, H., Braig, K., and Saibil, H. R. (1996) *Cell 87*, 241−251.
8. Saibil, H. R., Zheng, D., Roseman, A. M., Hunter, A. S., Watson, G. M. F., Chen, S., auf der Mauer, A., O'Hara, B. P., Wood, S. P., Mann, N. H., Barnett, L. K., and Ellis R. J. (1993) *Curr. Biol. 3*, 265−273.
9. Chen, S., Roseman, A. M., Hunter, A. S., Wood, S. P., Burston, S. G., Ranson, N. A., Clarke, A. R., and Saibil, H. R. (1994) *Nature 371*, 261−264.
10. Ranson, N. A., White, H. E., and Saibil, H. R. (1998) *Biochem. J. 333*, 233−242.
11. White, H. E., Chen, S., Roseman, A. M., Yifrach, O., Horovitz, A., and Saibil, H. R. (1997) *Nat. Struct. Biol. 4*, 690−694.
12. Braig, K., Otwinowski, Z., Hegde, R., Boisvert, D. C., Joachimiak, A., Horwich A. L., and Sigler, P. B. (1994) *Nature 371*, 578−586.
13. Braig, K., Adams, P. D., and Brünger, A.T. (1995) *Nat. Struct. Biol. 2*, 1083−1094.
14. Hunt, J. F., Weaver, A. J., Landry, S. J., Gierasch, L., and Deisenhofer, J. (1996) *Nature 379*, 37−45.
15. Xu, Z., Horwich, A. L., and Sigler, P. B. (1997) *Nature 388*, 741−750.
16. Rye, H. S., Burston, S. G., Fenton, W. A., Beechem, J. M., Xu, Z., Sigler, P. B., and Horwich, A. L. (1997) *Nature 388*, 792−798.
17. Sparrer, H., and Buchner, J. (1997) *J. Biol. Chem. 272*, 14080−14086.
18. Lorimer, G. (1997) *Nature 388*, 720−723.
19. Sparrer, H., Lilie, H., and Buchner, J. (1996) *J. Mol. Biol. 258*, 74−87.
20. Viitanen, P. V., Gatenby, A. A., and Lorimer, G. H. (1992) *Protein Sci. 1*, 363−369.
21. Ewalt, K. L., Hendrick, J. P., Houry, W. A., and Hartl, F.-U. (1997) *Cell 90*, 491−500.
22. Gray, T. E., and Fersht, A. R. (1993) *J. Mol. Biol. 232*, 1197−1207.
23. Hutchinson, J. P., El-Thaher, T. S. H., and Miller, A. D. (1994) *Biochem. J. 302*, 405−410.
24. Okazaki, A., Ikura, T., Nikaido, K., and Kuwajima, K. (1994) *Nat. Struct. Biol. 1*, 439−446.
25. Hayer-Hartl, M. K., Ewbank, J. J., Creighton, T. E., and Hartl, F.-U. (1994) *EMBO J. 13*, 3192−3202.
26. Flynn, G. C., Beckers, C. J. M., Baase, W. A., and Dahlquist, F. W. (1993) *Proc. Natl. Acad. Sci. U.S.A. 90*, 10826−10830.
27. Lilie, H., and Buchner, J. (1995) *Proc. Natl. Acad. Sci. U.S.A. 92*, 8100−8104.
28. Smith, K. E., and Fisher, M. T. (1995) *J. Biol. Chem. 270*, 21517−21523.
29. Katsumata, K., Okazaki, A., Tsurupa, G. P., and Kuwajima, K. (1996) *J. Mol. Biol. 264*, 643−649.
30. Robinson, C. V., Groβ, M., Eyles, S. J., Ewbank, J. J., Mayhew, M., Hartl, F.-U., Dobson, C. M., and Radford, S. E. (1994) *Nature 372*, 646−651.
31. Okazaki, A., Katsumata, K., and Kuwajima, K. (1997) *J. Biochem. 121*, 534−541.
32. Gervasoni, P., Gehrig, P., and Plückthun, A. (1998) *J. Mol. Biol. 275*, 663−675.
33. Gervasoni, P., Staudenmann, W., James, P., Gehrig, P., and Plückthun, A. (1996) *Proc. Natl. Acad. Sci. U.S.A. 93*, 12189−12194.
34. Nieba-Axmann, S. E., Ottiger, M., Wuthrich, K., and Plückthun, A. (1997) *J. Mol. Biol. 271*, 803−818.
35. Zahn, R., Perrett, S., Stenberg, G., and Fersht, A. R. (1996) *Science 271*, 642−645.
36. Torella, C., Mattingly, J. R., Jr., Artigues, A., Iriarte, A., and Martinez-Carrion, M. (1998) *J. Biol. Chem. 273*, 3915−3925.
37. Richarme, G., and Kohiyama, M. (1994) *J. Biol. Chem. 269*, 7095−7098.
38. Brazil, B. T., Cleland, J. L., McDowell, R. S., Skelton, N. J., Paris, K., and Horowitz, P. M. (1997) *J. Biol. Chem. 272*, 5105−5111.
39. Buckle, A. M., Zahn, R., and Fersht, A. R. (1997) *Proc. NatI. Acad. Sci. U.S.A. 94*, 3571−3575.
40. Dessauer, C. W., and Bartlett, S. G. (1994) *J. Biol. Chem. 269*, 19766−19776.
41. Landry, S. J., and Gierasch, L. M. (1991) *Biochemistry 30*, 7359−7362.
42. Landry, S. J., Jordan, R., McMacken, R., and Gierasch, L. M. (1992) *Nature 355*, 455−457.
43. Rosenberg, H. F., Ackerman, S. J., and Tenen, D. G. (1993) *J. Biol. Chem. 268*, 4499−4503.
44. Mattingly, J. R., Jr., Iriarte, A., and Martinez-Carrion, M. (1995) *J. Biol. Chem. 270*, 1138−1148.
45. Hlodan, R., Tempst, P., and Hartl, F.-U. (1995) *Nat. Struct. Biol. 2*, 587−595.
46. Hoshino, M., Kawata, Y., and Goto, Y. (1996) *J. Mol. Biol. 262*, 575−587.
47. Clark, A. C., Hugo, E., and Frieden, C. (1996) *Biochemistry 35*, 5893−5901.
48. Itzhaki, L. S., Otzen, D. E., and Fersht, A. R. (1995) *Biochemistry 34*, 14581−14587.
49. Katsumata, K., Okazaki, A., and Kuwajima, K. (1996) *J. Mol. Biol. 258*, 827−838.
50. Perrett, S., Zahn, R., Stenberg, G., and Fersht, A. R. (1997) *J. Mol. Biol. 269*, 892−901.
51. Fenton, W. A., Kashi, Y., Furtak, K., and Horwich, A. L. (1994) *Nature 371*, 614−619.
52. Schmidt, M., and Buchner, J. (1992) *J. Biol. Chem. 267*, 16829−16833.
53. Gierasch, L. M., Wang, Z., Hunt, J., Landry, S. J., Weaver, A., and Deisenhofer, J. (1995) *Protein Eng.* (*Suppl.*) *8*, 14.
54. Shimizu, A., Tanba, T., Ogata, I., Ikeguchi, M., and Sugai, S. (1998) *J. Biochem. 124*, 319−325.
55. Zahn, R., and Plückthun, A. (1994) *J. Mol. Biol. 242*, 165−174.
56. Walter, S., Lorimer, G. H., and Schmid, F. X. (1996) *Proc. Natl. Acad. Sci. U.S.A. 93*, 9425−9430.
57. Buchner, J. (1996) *FASEB J. 10*, 10−19.
58. Miller, A. D., Maghlaoui, K., Albanese, G., Kleinjan, D. A., and Smith, C. (1993) *Biochem. J. 291*, 139−144.
59. Tabona, P., Reddi, K., Khan, S., Nair, S. P., Crean, St. J. V., Meghji, S., Wilson, M., Preuss, M., Miller, A. D., Poole, S., Came, S., and Henderson, B. (1998) *J. Immunol. 161*, 1414−1421.
60. Yang, J. J., and van Wart, H. E. (1994) *Biochemistry 33*, 6508−6515.
61. Benesi, H. A., and Hildebrand, J. H. (1949) *J. Am. Chem. Soc. 71*, 2703−2707.
62. Price, N. C., Kelly, S. M., Wood, S., and auf der Mauer, A. (1991) *FEBS Lett. 292*, 9−12.
63. Hayer-Hartl, M. K., and Hartl, F.-U. (1993) *FEBS Lett. 320*, 83−84.
64. Ybarra, J., and Horowitz, P. M. (1995) *J. Biol. Chem. 270*, 22962−22967.
65. Blennow, A., Surin, B. P., Ehring, H., McLennan, N. F., and Spangfort, M. D. (1995) *Biochim. Biophys. Acta 1252*, 69−78.
66. Burston, S. G., Ranson, N. A., and Clarke, A. R. (1995) *J. Mol. Biol. 249*, 138−152.
67. Zhang, X., Chen, L., Bancroft, D. P., Lai, C. K., and Maione, T. E. (1994) *Biochemistry 33*, 8361−8366.
68. Abrecht, C., Müller, K., Obrecht, D., and Trzeciak, A. (1995) F. Hoffmann-La Roche AG European Patent No. 0640618A1.
69. DeGrado, W. F., and Lear, J. D. (1985) *J. Am. Chem. Soc. 107*, 7684−7689.
70. Altmann, K.-H., and Mutter, M. (1990) *Int. J. Biochem. 22*, 947−956.
71. Cohen, C., and Parry, D. A. D. (1994) *Science 263*, 488−489.
72. Lee, J. C., and Timasheff, S. N. (1977) *Biochemistry 16*, 1754−1764.
73. Hemmingsen, S. M., Woolford, C., van der Vies, S. M., Tilly, K., Dennis, D. T., Georgopoulos, C. P., Hendrix, R. W., and Ellis, R. J. (1988) *Nature 333*, 330−334.

74. Behlke, J., Ristau, O., and Schönfeld, H.-J. (1997) *Biochemistry 36*, 5149−5156.
75. Hayer-Hartl, M. K., Martin, J., and Hartl, F.-U. (1995) *Science 269*, 836−841.
76. Kawata, Y., Hongo, K., Nosaka, K., Furutsu, Y., Mizobata, T., and Nagai, J. (1995) *FEBS Lett. 369*, 283−286.
77. Todd, M. J., Viitanen, P. V., and Lorimer, G. H. (1993) *Biochemistry 32*, 8560−8567.
78. Llorca, O., Marco, S., Carrascosa, J. L., and Valpuesta, J. M. (1997) *FEBS Lett. 405*, 195−199.
79. Kad, N. M., Ranson, N. A., Cliff, M. J., and Clarke, A. R. (1998) *J. Mol. Biol. 278*, 267−278.
80. Yifrach, O., and Horovitz, A. (1998) *Biochemistry 37*, 7083−7088.
81. Yifrach, O., and Horovitz, A. (1996) *J. Mol. Biol. 255*, 356−361.
82. Sturtevant, J. M. (1977) *Proc. Natl. Acad. Sci. U.S.A. 74*, 2236−2240.
83. Ha, J.-H., Spolar, R. S., and Record, M. T., Jr. (1989) *J. Mol. Biol. 209*, 801−816.
84. Kresheck, G. C., Vitello, L. B., and Erman, J. E. (1995) *Biochemistry 34*, 8398−8405.
85. Lin, Z., Schwarz, F. P., and Eisenstein, E. (1995) *J. Biol. Chem. 270*, 1011−1014.
86. Aoki, K., Taguchi, H., Shindo, Y., Yoshida, M., Ogasahara, K., Yutani, K., and Tanaka, N. (1997) *J. Biol. Chem. 272*, 32158−32162.
87. Staniforth, R. A., Burston, S. G., Atkinson, T., and Clarke, A. R. (1994) *Biochem J. 300*, 651−658.
88. Tsurupa, G. P., Ikura, T., Makio, T., and Kuwajima, K. (1998) *J. Mol. Biol. 277*, 733−745.
89. Pajot, P. (1976) *Eur. J. Biochem. 63*, 263−269.

BI990342L